

Raman-scattering evidence for free spinons in the one-dimensional spin- $\frac{1}{2}$ chains of Sr_2CuO_3 and SrCuO_2

O. V. Misochko* and S. Tajima

Superconductivity Research Laboratory, ISTEK, Koto-ku, Tokyo 135, Japan

C. Urano, H. Eisaki, and S. Uchida

Department of Applied Physics, University of Tokyo, Tokyo 113, Japan

(Received 21 February 1996)

The Raman scattering of single crystals Sr_2CuO_3 and SrCuO_2 is investigated under resonant conditions. Of all polarizations, only the Raman spectrum with the electrical vector along the CuO chains shows additional peaks superimposed on a strong continuum. Three of the peaks and the continuum demonstrate unconventional temperature dependence. These additional features are ascribed to either the phonons coupled to a resonating valence bond, or to the pairs of unbound spinons that resonate as the excitation energy approaches the charge-transfer gap. The additional scattering cannot be explained by excitations out of a long-range ordered state but is consistent with that expected for either free spinon pairs or spin-liquid-state excitations.

[S0163-1829(96)51322-6]

Recently there has been great interest in spin-ladder structures $\text{Sr}_{n-1}\text{Cu}_{n+1}\text{O}_{2n}$ consisting of the parallel line of CuO double chains periodically intergrown within the CuO_2 sheets. According to theoretical predictions these structures, composed of $(n-1)/2$ -leg ladders, are either a frustrated gapped quantum antiferromagnet for odd n , or a gapless one for even n .^{1,2} The infinite chains Sr_2CuO_3 (Sr213) and SrCuO_2 (Sr112), appearing as structure blocks in the spin-ladder materials, have been reported to be the one-dimensional, spin- $\frac{1}{2}$, Heisenberg antiferromagnet with the exchange constant $J \approx 1000$ K.^{3,4} However, the nature of the ground state and that of the elementary excitations in these materials has not been so far addressed. recent study of the spin- $\frac{1}{2}$ chain KCuF_3 has demonstrated that elementary excitations in this one-dimensional (1D) system have fermion character in contrast to a boson character expected for an ordered ground state.⁵ Therefore, the investigation of Sr_2CuO_3 and SrCuO_2 , that are the best realization of one-dimensional system,⁴ would be indispensable both for a description of the $\text{Sr}_{n-1}\text{Cu}_{n+1}\text{O}_{2n}$ system and a better understanding of the 1D magnetic systems. Previous Raman studies of solid solutions of $\text{Ca}_{2-x}\text{Sr}_x\text{CuO}_3$ have revealed a rich structure of the Raman spectra for the light polarized along the chain.^{6,7} The authors tried to explain it either by the first order phonon scattering from zone boundary⁶ or by second-order scattering.⁷ In both cases, disorder was considered to be the primary reason for appearance of the forbidden peaks. The disorder does exist in the solid solutions, mainly on the metal ion lattice, $\text{Sr} \leftrightarrow \text{Ca}$ disorder, but it is expected to disappear in the stoichiometric materials like Sr213 and Sr112.

Herein we report an optical study of Sr213 and Sr112 single crystals. From the optical study we deduce that there is a charge transfer gap for the in-chain polarization where the Raman spectra show a rich structure superimposed on a strong continuum. In this paper we propose an interpretation for the rich structure and wide range continuum based on their temperature and resonant behavior. We show that some

of the peculiarities can be qualitatively explained as a result of the specific spin-spin and/or spin-phonon interaction signaling a non-bosonic nature of the elementary excitations.

Single crystals of Sr213 and Sr112 were grown by a traveling-solvent-zone technique and had dimensions up to $10 \times 5 \times 5$ mm³. In the crystal structures, shown in insets of Fig. 1, of important are Cu ions coordinated with four oxygen ones forming infinite CuO chains along the copper-bridging oxygen direction. In Sr112 the second chain is displaced by half the lattice constant. Throughout the paper we use the laboratory coordinate system with y axis running along the chains and z axis along the apical oxygen direction.

The crystals were oriented using an x-ray diffractometer and polished with a diamond paste. The reflectivity measured with a Hitachi grating-type spectrometer in different polarizations revealed strong transitions peaked around 2 eV for the light polarized along chains, all other polarizations being featureless. The Raman spectra were taken using a JY6400 triple spectrometer with a CCD multichannel detector in a pseudoback scattering configuration. For low temperature measurements the crystals were mounted on the cold finger of a He-flow UHV cryostat. For high energy spectra, we used the last spectrograph of our Raman system, equipped with 150 grooves/mm grating, eliminating the laser line with a notch filter. The resonant profiles were investigated at room temperature by using the discrete lines of an Ar^+/Kr^+ laser. All spectra were corrected for the optical system response and normalized for laser power.

In Fig. 1 we show a set of three polarized Raman spectra at the yellow excitation for Sr213 and Sr112, respectively. While the zz spectra for both crystals show only the phonons expected from a factor group analysis, there are additional broad and strong peaks in the yy spectra which are shown in more detail in Fig. 2. These peaks are superimposed on a broad background extending up to 7000 cm⁻¹ as demonstrated in Fig. 3. The peaks with an energy higher than 1500 cm⁻¹ are relatively weak, and the mode centered around 1650 cm⁻¹ in Sr213 is a doublet in contrast to Sr112. By changing the excitation, we found that the sharp phonons in

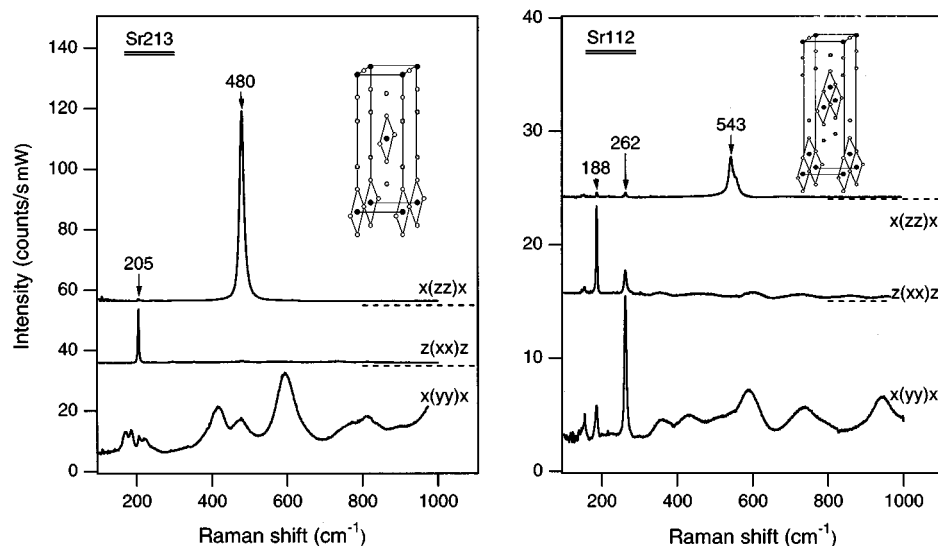


FIG. 1. Raman spectra of the Sr213 (left panel) and Sr112 (right panel) single crystals obtained at the yellow excitation. Baseline for the bottom spectrum in each panel is the x axis; baselines for the two top spectra are shown in dashed lines. The insets in each panel show crystal structure of the sample investigated.

the xx polarization do not resonate, while those in the zz polarization resonate differently (they are peaked at 2.5 eV) as compared to the peaks in the yy geometry resonating toward 2 eV. The continua also show resonant behavior, their intensity increasing toward the red (see insets of Fig. 2). Additionally, tuning the incident photon frequency toward the charge-transfer gap, we observed not only the resonant enhancement of the most strong features, but a change in the center position as shown in the inset of Fig. 2 for Sr213. At low temperatures, three of the extra peaks in the yy spectra (around 600, 1000, and 1150 cm^{-1}) become stronger and sharper in both compounds, the continuum being suppressed at the low frequency side, as shown in Fig. 4 for Sr 213.

The factor group analysis predicts two A_g Raman active phonons (apical oxygen and strontium) in Sr213. There are also two more diagonal phonons in the double chain material

that arise from the z displacement of bridging oxygen and that of the Cu ion, the two becoming Raman active due to change of the site symmetry. Following the previous assignment for $\text{Ca}_{2-x}\text{Sr}_x\text{CuO}_3$,⁶ in Sr213 we ascribe the 480 cm^{-1} mode to apical oxygen vibration and the 205 cm^{-1} one to the vibration of Sr.

Frequencies, relative intensity, and polarization selection rules of the Raman allowed peaks in Sr112 are similar to those in Sr213. There are two A_g oxygen modes with almost degenerate frequencies (543 and 558 cm^{-1}) dominating the zz spectrum. An increase in frequency reveals that the chains become less rigid in the z direction as compared to the single chain material. One can expect that the two oxygen modes have a mixed character, both oxygen taking part in each of them. The Sr vibration shifts a bit to the low frequency side located now at 188 cm^{-1} . Additionally, the Cu ion vibration appears at 262 cm^{-1} .

We now dwell on the yy spectra. All the extra peaks here resonate when the laser energy approaches the charge-transfer gap, the resonance being stronger than that of the allowed phonons. A similar resonant behavior is observed for the continuum that features reside on. From Fig. 2 we can see that in the two materials the highest energy peaks centered at around 1150 cm^{-1} are asymmetric, the high energy

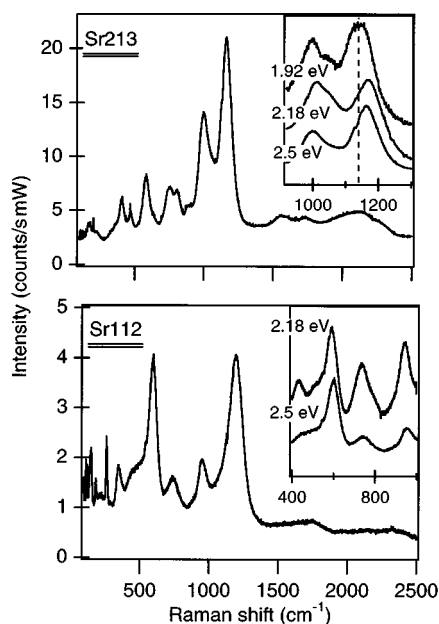


FIG. 2. The yy spectra of Sr213 (upper panel) and Sr112 (bottom panel) at the 497 nm excitation. The insets show resonant behavior for the two high energy features and continuum in each crystal. Baseline for all the spectra is the x axis.

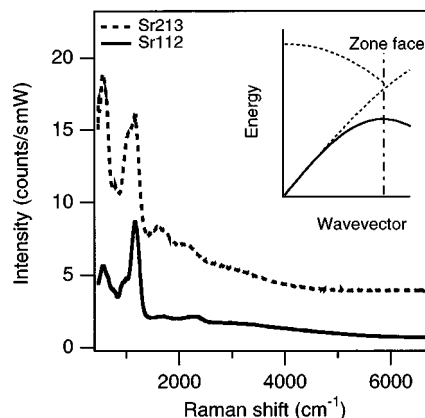


FIG. 3. High-energy spectra in the yy polarization for Sr213 and Sr112 at the green excitation. The inset shows a sketch of the dispersion for the lower bound (solid line) and upper bound of the continuum of two spinon states (dotted line).

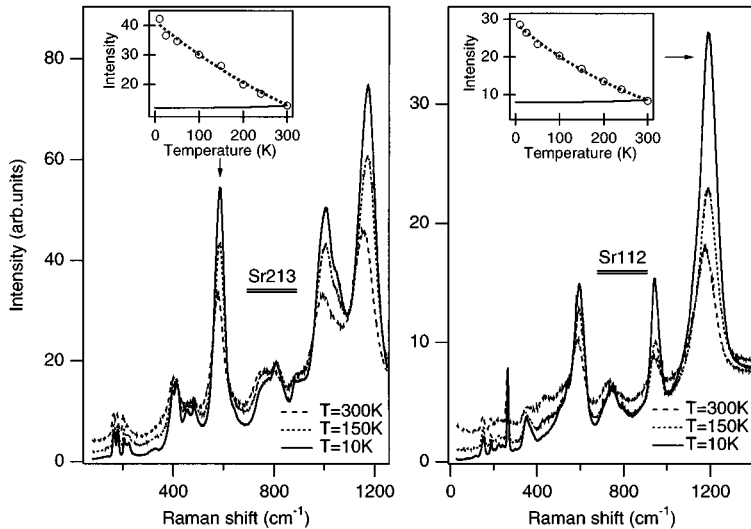


FIG. 4. Temperature dependence of the Raman scattering in the yy polarization for Sr213 (left panel) and Sr112 (right panel). The insets show the temperature dependence of peak intensity for the 580 cm^{-1} mode in Sr213 and for the 1180 cm^{-1} mode in Sr112. The solid lines are the expected temperature dependence for the first order and second order Raman scattering in Sr213 and Sr112, respectively.

slope being steeper than the low energy one. In addition, the feature at 1000 cm^{-1} in the Sr213 is a doubled peak that can be more clearly seen at low temperatures (Fig. 4) and under resonance (inset of Fig. 2). As the temperature is lowered the three features (around 600 , 1000 , and 1150 cm^{-1}) demonstrate an unexpected temperature dependence for phonons. Neither the peaked nor integrated intensity of the features, the latter obtained when fitted by a Lorentzian, follow the temperature dependence expected for either the first or second order scattering. Instead of decreasing with the temperature, we observed an increase in intensity. This can be seen in Fig. 4 and is illustrated in the inset for the 580 cm^{-1} mode of Sr213. The temperature dependence of the charge-transfer gap can hardly account for this effect—the increase due to resonant denominator may outweigh the decrease due to state population, but then the continuum would have resonated the same way. At the same time, the continuum's strength at low energy follows the temperature dependence expected for a second order scattering indicating that the excitations responsible for the scattering have acoustical dispersion.

Assuming all the peaks are phonons, we attempted to explain the rich structure of the spectrum by disorder induced scattering, Peirls instability, and Fröhlich-interaction induced longitudinal phonons. None of these explanations could satisfy the experimental data. For instance, the disorder, even if it existed, must affect all polarizations. The same applies to the Peirls induced unit cell doubling that may lead to additional phonons. The Fröhlich interaction induced scattering can result in the forbidden longitudinal phonons. It may have been the reason for the extra features, but in our 1D case it is not possible to create the longitudinal phonon propagating along the chain either in the $x(yy)x$ or $z(yy)z$ polarization. So, we are led to conjecture that all the peculiarities observed in this polarization may come from correlated behavior of the electrons; that is the motion of a single electron along the chain is correlated with that of others. Thus the peculiarity of the yy polarization is a manifestation of the 1D nature of the crystals. If the correlations do play a major role in the crystals under study, their state may be a spin liquid⁸ with its specific excitations.⁹ Consequently, to understand Raman scattering we have to take into account coupling of a phonon to singlet pairs. In such a scenario we

divide phonons into two types—those coupled to an exchange term and those which are uncoupled. Since exchange between the Cu ions is mediated by the oxygen midway between them, the most plausible candidates for the exchange coupled phonons are the modes originated from the movement of bridging oxygen: for instance, the stretching and bending modes (O_1 and O_2 , respectively, from here on). From the infrared study of $\text{Ca}_{2-x}\text{Sr}_x\text{CuO}_3$,^{6,7} we know that their frequencies are around 600 and 400 cm^{-1} , and that they are almost the same frequencies as those of two of the extra peaks. Besides, as it has been shown by Kivelson *et al.*,⁹ in a spin-liquid state the lattice deformation (phonon) associated with spinon stabilizes the spin-liquid state with respect to the Néel state. Hence appearance of these phonons in the Raman scattering may be an evidence for the spin-liquid state and considered as a manifestation of hybrid nature of the resonating valence bond (spinon plus phonon).

Trying to make the phonon assignment for Sr213, we can relate the 580 and 408 cm^{-1} peaks to O_1 and O_2 modes, the 750 and 1160 cm^{-1} features to their overtones, and the 1000 cm^{-1} peak to a combination O_1+O_2 . The two phonon peaks have linewidths roughly twice as large as the one-phonon ones. In a similar way, going to double chain crystal, the 605 and 350 cm^{-1} peaks can be assigned to O_1 and O_2 phonons, the 1190 and 740 cm^{-1} to their overtones, and the 950 cm^{-1} feature to their sum. However, within the phonon assignment it is not possible to explain the strong continuum extending over 7000 cm^{-1} and peculiar temperature dependence for the three most pronounced modes.

Another possible explanation of the spectrum is that the most pronounced peaks demonstrating unusual temperature dependence can be ascribed to spinon pairs states. Unlike Haldane systems where spinons are bound, in the linear spin- $\frac{1}{2}$ chain they are free.¹⁰ The spinons have semionic statistics^{10,11} and their wave vector is restricted within half of the Brillouin zone. The low excited states for the spin- $\frac{1}{2}$ linear system are the spin waves which can be reduced to a superposition of two spinons.^{10,11} When the spinons are unbound, there is a continuum of the spinon pair states for each wave vector with the high-energy cutoff corresponding to the pair of spinons the half wave vector each.¹⁰⁻¹² The dispersion of the spin wave together with the upper bound of the spinon pair continuum is schematically shown in the inset of

Fig. 3. In the magnetic assignment we have two modes coming from the edge of the Brillouin zone where the density of states is large due to flatness of the dispersion curves (the 600 cm^{-1} peak would correspond to the low bound of the paired spinon state, the one around 1000 cm^{-1} being the upper bound of the continuum at the same wave vector). One more mode at the Γ point, the highest energy feature, arises due to upper bound of the continuum; see the inset of Fig. 3. In this case, asymmetry of the peaks and the doubled peak at the 1000 cm^{-1} can be easily explained by finite wave vector scattering.¹³ The change of the peak position and line shape with excitation finds a natural explanation along the same finite wave vector line. The magnetic assignment is not favored by the fact that the three above-mentioned features are peaked at the energies which do not coincide with those expected from theory.¹¹ However, the features centered at around 1100 , 1650 , and 2300 cm^{-1} correspond to the theory expectation and can, therefore, as well be plausible candidates for spin pair states.

Accepting the magnetic assignment, unusual temperature dependence of the most pronounced peaks ceases to be mysterious. There are two facts strongly suggesting that ground state of the system is a spin liquid (that is the elementary excitations are nonbosonic). First, the modes are sharp even far away from the ordered state that has been found around 8 and 2 K in Sr213 and Sr112, respectively.^{3,14} Secondly, the experimental spectra do not coincide with that expected from the Néel ground state in which there should be only a single two magnon peak even if the magnon is overdamped. Our explanation and experimental evidence are in good agreement with the unbound spinons results⁵ obtained for KCuF_3 . Unfortunately, only a few features of the spectra can be explained within the magnetic assignment; the rest would require phonons. However, with the present experimental data, it is not possible to select between the phonon and magnetic assignments. They can be both at work and only their combination would provide an ultimate description of the complicated spectra.

We should mention here that similar combination of the forbidden peaks has been commonly observed in the insulators of high- T_c materials such as La_2CuO_4 ,¹⁵ $(\text{Ca,Sr})\text{CuO}_2$,¹⁵ $\text{YBa}_2\text{Cu}_3\text{O}_6$,^{15,16} $\text{Pb}_2\text{Sr}_2\text{PrCu}_3\text{O}_8$,¹⁷ which are considered to be strongly correlated systems, and as well as in one-dimensional $\text{Ca}_{2-x}\text{Sr}_x\text{CuO}_3$,^{6,7} where the correlations are strong. In most cases the forbidden peaks reside on a continuum and a spin-liquid state has been considered as a plausible candidate for the ground state. Thus our conjecture that

the additional scattering is due to correlation effects or frustrated interaction which turn the system into the spin liquid seems to be plausible.

The enhanced Raman intensity for the additional scattering is likely to come from correlation effects amplified by reduced dimensionality of the system. It has been known that the second order scattering, in a strongly correlated system, is limited to wave vectors smaller than the inverse exciton Bohr radius.¹⁸ For semiconductors, where the exciton is of Wannier type, this restricts the Raman scattering to probing dispersion only near the Γ point. In charge-transfer insulators like antiferromagnetic phase of the high- T_c oxides and one-dimensional system under current investigation, the charge-transfer exciton is of small radius because of its nature. Indeed, there has even been an attempt to explain the charge-transfer exciton in the high- T_c materials as a Frenkel one.¹⁹ Therefore, the Raman scattering in such a system it is possible to probe a larger part of the Brillouin zone thus contributing to the enhanced scattering.

In a narrow band system light can couple to an electron either through a resonant process (coupled to the current) and/or by a nonresonant one (coupled to the inverse mass tensor).²⁰ It is quite natural to expect that in our insulating case the former would dominate. From the temperature dependence and resonant enhancement, we can conclude that dominant contribution to the continuum is a resonant process due to light coupling to spin pairs. Because the elementary excitations in spin liquid are topological defects they appear as spectroscopic particles only in pairs (spinon-spinon). Moreover, the dispersion of the excitations responsible for the continuum must be acoustical (no gap). A crucial test to distinguish between the phonon stabilized and pure spin-liquid state is to determine nature of the strong peaks with anomalous temperature behavior. It can be most easily done by oxygen isotope substitution.

In conclusion, we have measured the Raman scattering of linear spin- $\frac{1}{2}$ antiferromagnets Sr213 and Sr112. The sharp features observed in the polarized spectra have been assigned to diagonal phonons. A number of the peaks pronounced for the in-chain polarization has been ascribed either to the phonons strongly coupled to spinons or to the spinon-spinon pairs. The additional scattering cannot be understood assuming excitations out of a long-range ordered ground state which leads us to a natural explanation in terms of the excitations of nonbosonic nature.

The authors gratefully acknowledge E. Ya. Sherman for helpful comments and S. S. Rao for critical reading of the manuscript.

*Permanent address: Institute of Solid State Physics, Russian Academy of Sciences, 142432 Chernogolovka, Russia.

¹S. Gopalan *et al.*, Phys. Rev. B **49**, 8901 (1994).

²S. R. White *et al.*, Phys. Rev. Lett. **73**, 886 (1994).

³T. Ami *et al.*, Phys. Rev. B **51**, 5994 (1995).

⁴N. Motoyama *et al.*, Phys. Rev. Lett. **76**, 3212 (1996).

⁵D. A. Tennant *et al.*, Phys. Rev. Lett. **70**, 4003 (1993).

⁶M. Yoshida *et al.*, Phys. Rev. B **44**, 11 997 (1991).

⁷G.A. Zlateva *et al.*, J. Phys. Condens. Matter **4**, 8543 (1992).

⁸P.W. Anderson, Mater. Res. Bull. **8**, 153 (1973).

⁹S. A. Kivelson *et al.*, Phys. Rev. B **35**, 8865 (1987).

¹⁰L. D. Faddeev and L. A. Takhtajan, Phys. Lett. **85A**, 375 (1981).

¹¹F. D. Haldane and M. R. Zirnbauer, Phys. Rev. Lett. **71**, 4055 (1993).

¹²G. Müller *et al.*, Phys. Rev. B **24**, 1429 (1981).

¹³O. V. Misochko and E. Ya. Sherman, Physica C **222**, 219 (1994).

¹⁴K. Kojima *et al.* (unpublished).

¹⁵M. Yoshida *et al.*, Phys. Rev. B **46**, 6505 (1992).

¹⁶E. T. Heyen *et al.*, Phys. Rev. B **45**, 30 337 (1992).

¹⁷M. Reddyk *et al.*, Phys. Rev. B **50**, 13 762 (1994).

¹⁸J. F. Scott *et al.*, Phys. Rev. **188**, 1285 (1969).

¹⁹V. I. Belincher *et al.*, Phys. Rev. B **50**, 13 768 (1994).

²⁰Y. Bang, Physica C **218**, 251 (1993).